Korean J. Chem. Eng., **27**(6), 1689-1694 (2010)
DOI: 10.1007/s11814-010-0292-6

Enhancement of oxygen reduction activity by sequential impregnation of Pt and Pd on carbon support

Dohwa Jung*, Sangchul Beak*, Kee Suk Nahm*,, and Pil Kim*,**,†**

*Department of Hydrogen and Fuel Cell Engineering, Specialized Graduate School, Chonbuk National University, Jeonju 561-756, Korea
**School of Semiconductor and Chemical Engineering, Chonbuk National University, Jeonju 561-756, Korea
(*Received 15 October 2009 • accepted 9 March 2010*)

Abstract−Two Pd-based PtPd bimetallic catalysts (mole ratio of Pt to Pd=1 : 18) were prepared by co-impregnation (Pt-Pd/C) and sequential impregnation of Pt on Pd/C [Pt(Pd/C)] for the application to oxygen reduction reaction (ORR). The prepared bimetallic catalysts had lower ORR activities than Pt/C, while they showed largely enhanced activity compared to Pd/C. In particular, the extent of enhancement was found to be dependent on the surface composition. The observed mass and specific activities of Pt(Pd/C) were more than two times higher than those of Pt-Pd/C. The superior activity of Pt(Pd/C) observed from the performed studies was attributed to its Pt-rich surface.

Key words: Oxygen Reduction Reaction (ORR), Pd Catalyst, Pt Catalyst, Bimetallic Catalyst, Polymer Electrolyte Fuel Cells (PEMFCs)

INTRODUCTION

Polymer electrolyte fuel cells (PEMFCs) have attracted much attention as primary power sources for zero-emission electric vehicles due to their high energy conversion efficiency and environmental friendly nature. Though there have been many efforts devoted to the technical advancements of PEMFCs on the last decades, several barriers still remain to be overcome for the commercialization of PEMFCs [1-4].

One of them is a sluggish kinetics for oxygen reduction reaction (ORR) at cathode. This induces a large amount of Pt-based metal catalyst utilization, increasing the overall cost of fuel cells. The cost will be effectively reduced either by improving the catalytic activity of Pt catalyst or developing an alternative low-cost catalyst.

Heat-treated metal-porphyrin, in which metal ions such as Co and Fe are bound to nitrogen in carbon structure, has been proposed as an effective alternative cathode catalyst [5-7]. Although the materials may be abundant in nature and consequently can be supplied at lower price, their catalytic activity and stability are currently insufficient for the cathode catalyst utilization.

As a typical method to enhance ORR performance, Pt has been alloyed with transition metals such as Co [8], Ni [3], Fe [9], Ti [10], and Cu [11]. Toda et al. have prepared several Pt alloys with Ni, Co, and Fe using a sputtering method and investigated the several factors which affect the electrocatalytic activity of the catalysts [12]. They reported that Pt-based alloys had 10-15 times higher kinetic current than Pt, depending on the composition of catalysts. The obtained higher kinetic current was attributed to the increased d-electron vacancy of Pt surface layer. Stamenokovic et al. have recently reported an important result on the activity of Pt-based alloy [3]. They demonstrated that the activity of Pt (111) could be enhanced by alloying with Ni, resulting from the modified electronic configuration of surface Pt atom. The interaction between resultant modified Pt surface and oxide species such as hydroxide would be weakened, leaving active site for ORR unpoisoned, which resulted in 90-fold increased activity over a conventional Pt/C. There have been also interesting reports on the catalytic properties of Pt or Pt-M (M= Au, Rh, Ru, etc.) monolayer on Pd (111) [13,14]. The significant enhancement of ORR kinetics is not only due to the geometric effect such as increased surface roughness, but also to a decreased formation of PtOH. This resulted from the modified electronic structure of Pt surface. As can be seen from these examples, it is likely that the deposition of Pt on suitable metal surface such as Pd would be a promising method to increase ORR activity, and therefore to reduce Pt loadings in PEMFCs. In addition, the PtPd binary catalyst would be more economical than Pt monometallic one when considering the cost of metal. Currently, the price of Pd is about a third of that of Pt.

In this work, we prepared carbon-supported PtPd bimetallic catalysts by using a co-impregnation and a sequential impregnation method, respectively. The physico-chemical properties of catalysts were characterized by using XRD, TEM, XPS, and electrochemical methods and were correlated with ORR performances observed in acid solution.

EXPERIMENTAL

1. Materials

Pd and Pt precursors (Na_2PdCl_4 and H_2PtCl_6) were purchased from Aldrich and Kojima Chemicals, respectively. $NaBH_4$ (Aldrich) was used for a reducing agent for metal ions and Vulcan XC 72R (Cabot) for a catalyst support. Nafion solution (5 wt%) and isopropyl alcohol (IPA) were obtained from Aldrich and sulfuric acid (H_2SO_4, 98%) from Showa Chemical. Doubly distilled water was used in this study.

†To whom correspondence should be addressed.
E-mail: kimpill@chonbuk.ac.kr

2. Preparation of Catalysts

Two bimetallic catalysts, Pt-Pd/C and Pt(Pd/C), were prepared using $NaBH_4$ reducing agent by a co-impregnation and sequential impregnation, respectively. For the preparation of Pt-Pd/C, carbon support (200 mg) was dispersed in a mixed solution of Na_2PdCl_4 (0.34 M, 2.38 ml) and H_2PtCl_6 (0.196 M, 0.23 ml). After making the above solution homogeneous through magnetic stirring followed by sonication, an aqueous solution of $NaBH_4$ (0.048 M, 50 ml) was added slowly to the solution under vigorous stirring. After further stirring for 1 h, a resultant precipitate was washed with copious water followed by drying at 110 °C for 6 h to produce the Pt-Pd/C. For the case of Pt(Pd/C), 30 wt% Pd/C was first prepared by the same method as Pt-Pd/C without the addition of Pt precursor. Prepared Pd/C was then dispersed in an aqueous solution of H_2PtCl_6 (0.196 M, 16 ml), followed by reduction of Pt on Pd/C using $NaBH_4$. The concentrations of Pt and Pd in two bimetallic catalysts were 3 wt% and 30 wt%, respectively. For the purpose of comparison, 30 wt% Pt/C was prepared by the same method used to prepare the Pd/C catalyst.

3. Characterizations and Measurement of ORR Performance

Crystalline phases of catalysts were identified by XRD (Rigaku D/MAX 2500) measurements using Cu-Kα radiation (λ=1.54056 Å) operated at 40 kV and 30 mA. The particle size and location of Pt on support were confirmed using TEM (JEOL-2010). Surface electronic states of elements in samples were examined with XPS (AXIS-NOVA (Kratos)).

To evaluate electrochemical active surface area and catalytic activity for ORR, electrochemical measurements were conducted with a conventional three-electrode cell in an electrolyte solution. A Pt gauze and a SCE were used as a counter electrode and a reference electrode, respectively. A working electrode was prepared by coating a catalyst ink on a glassy carbon (GC) electrode. For the preparation of catalyst ink, a catalyst (20 mg) was mixed with a few drops of water, IPA (8 ml) and Nafion (75 μl) solution. A repeated stirring followed by sonication to this catalyst slurry was carried out for 1 h to obtain a homogeneous catalyst ink. Cyclic voltammetry was conducted in a N_2 saturated H_2SO_4 (0.5 M) solution. Cyclic voltammograms (CV) of 10 cycles were recorded using CHI700C in the potential range of 0.1 to 1.2 V (vs. RHE) with a scan rate of 50 mV/s. For the estimation of ORR performance, linear sweep voltammetry (LSV) was carried out with a rotating ring disk electrode (RRDE, PINE (AFE7R9GCPT)) in oxygen saturated H_2SO_4 (0.5 M) solution. The working electrode was constructed with a catalyst ink-coated GC disk (diameter: 5.61 mm) and Pt ring. A linear sweep voltammogram was obtained in the potential range of 0.3-1.1 V (vs. RHE) with a scan rate of 5 mV/s. The metal loadings on GC electrode were 19 μg/cm^2 for Pd/C and 21 μg/cm^2 for Pt-Pd/C, Pt(Pd/C), and Pt/C.

RESULTS AND DISCUSSION

1. Physical Properties of Catalysts

Fig. 1 shows XRD patterns of Pd/C, Pt-Pd/C, Pt(Pd/C), and Pt/C catalysts. Three Pd-based catalysts reveal characteristic broad peaks at around 40, 46.5 and 68°, which respectively correspond to (111), (200), and (220) planes of Pd or PtPd bimetals with face-centered cubic crystalline phase [15]. While a similar diffraction pattern was observed with Pt/C, the characteristic peaks were shifted to lower angles. It was reported that the diffraction peaks for Pd in Pt_xPd_y alloys (x=1 and y=1-4) were observed to be shifted to a lower angles resulting from incorporation of Pt into Pd lattice, *i.e.*, lattice expansion of Pd [15]. In this work, however, it is hard to observe the evidence of lattice expansion. Compared to the bimetallic PtPd catalysts in the above reference, our bimetallic catalysts have very low Pt concentration; a mole ratio of Pt to Pd was kept at about 1 : 18. Because both Pt and Pd have an identical crystalline structure as well as a close atomic size to each other, the presence of small amount of Pt seems to have almost no effect on the lattice parameter of Pd in Pt-Pd/C and Pt(Pd/C) catalysts. A similar result to ours was reported in that a bimetallic Pt_xPd_y/C (x=1 and y=19) compared to Pd/C has no distinct feature in XRD pattern [16].

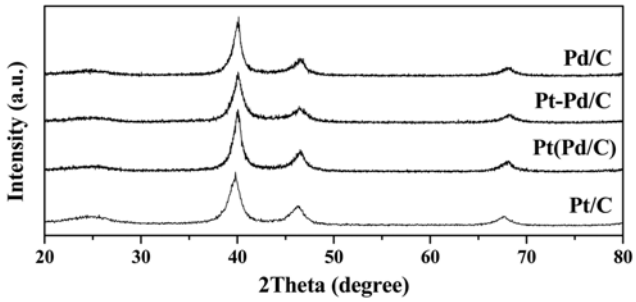

Fig. 1. XRD patterns of Pd/C, Pt-Pd/C, Pt(Pd/C), and Pt/C.

Table 1. Physical properties of Pd/C, Pt-Pd/C, Pt(Pd/C), and Pt/C

	Particle size (nm)		Surface area (m^2/g)[c]	Charge (mC/mg)[d]
	XRD[a]	TEM[b]		
Pd/C	5.7	5.8	87.7	48.5
Pt-Pd/C	5.4	5.7	86.4	48.1
Pt(Pd/C)	6.0	6.4	77.8	42.6
Pt/C	4.0	4.1	71.4	29.7

[a,c]Computed from XRD analyses
[b]Determined from TEM images
[d]Charge for the reduction of PdO on Pd/C, Pt-Pd/C, and Pt(Pd/C); Charge for the desorption of hydrogen on Pt/C

By applying the Scherrer equation to (220) reflection, the average particle size of metal was calculated as listed in Table 1. The bimetallic catalyst (Pt-Pd/C) had smaller crystallite size than the monometallic catalyst (Pd/C) when both catalysts were prepared by an impregnation method. This is probably because the growth of metal can be suppressed by the presence of different kind of metal ions. On the other hand, the average particle size of Pt(Pd/C) is slightly larger than that of Pd/C, indicating that the reduction of Pt ions was made predominately on the surface of Pd during the impregnation of Pt. In other words, the portion of independent presence of Pt apart from Pd would be very low in the Pt(Pd/C) catalyst. This is very important in designing a bimetallic catalyst because one metal has no influence on the electronic structure of the other metal if they are physically separated from each other. Metal surface area, as listed in Table 1, was calculated by using the following equation: Surface area (m^2/g)=6,000/rd, where r stands for the density of metal (Pt:

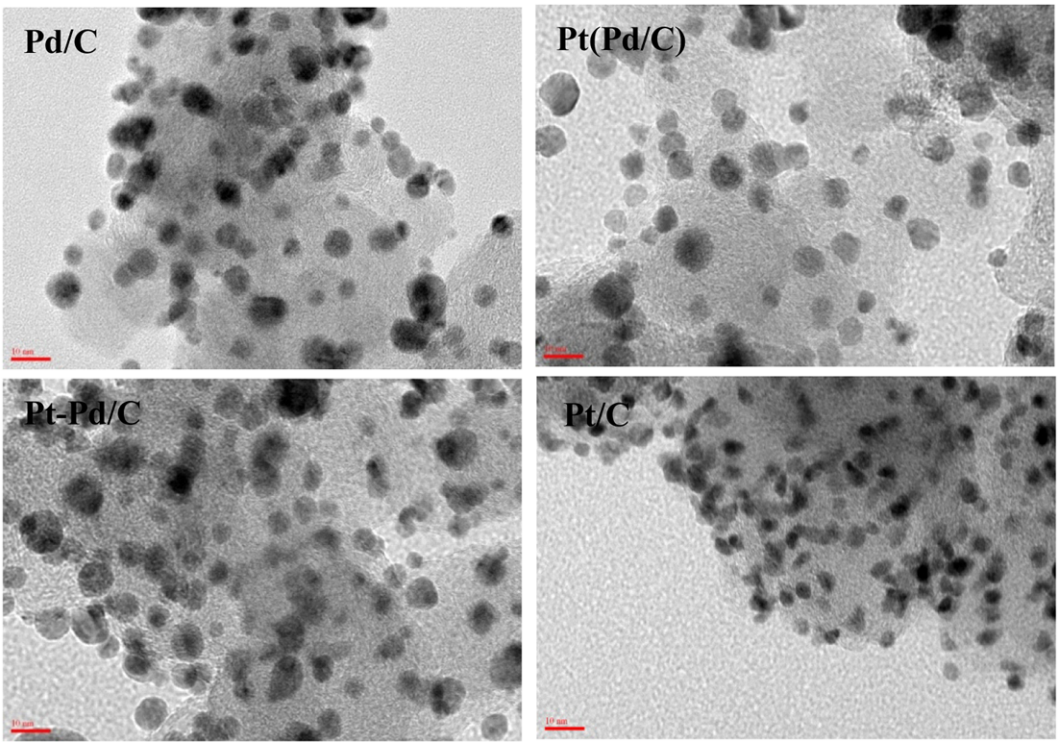

Fig. 2. TEM images of Pd/C, Pt-Pd/C, Pt(Pd/C), and Pt/C.

21.45 g/cm^3 and Pd: 12.02 g/cm^3) and d for particle size (nm). Metal surface area was 87.7, 86.4, 77.8, and 71.4 m^2/g for Pd/C, Pt-Pd/C, Pt(Pd/C), and Pt/C, respectively.

Fig. 2 shows TEM images of the catalysts. The particle size of the catalysts is similar to those observed from XRD. Average particle size was 5.8, 5.7, 6.4, and 4.1 nm for Pd/C, Pt-Pd/C, Pt(Pd/C), and Pt/C respectively.

To investigate the electronic state and surface concentrations of Pt, XPS analyses were conducted for two bimetallic catalysts and displayed in Fig. 3. The Pt $4f_{5/2}$ and $4f_{7/2}$ photoelectron lines were fitted into three components that can be assigned to zero-valent Pt, PtO, and PtO_2, respectively [17]. Table 2 summarizes the fitting results including binding energies and relative intensities for Pt species. A common feature of two bimetallic catalysts is that the binding energies for zero-valent Pt are slightly shifted to high binding energy compared to that of pure Pt (70.8 eV). This is usually observed on the supported Pt catalysts and is due to effects of small Pt cluster and Pt-support interaction [18]. Although the relative intensity of zero-valent Pt is fitter to be higher for Pt(Pd/C) than for Pt-Pd/C, its difference between two catalysts is unlikely to be significant because the fitting accuracy for Pt-Pd/C would not be as good as that for Pt(Pd/C) due to the considerable noise in the XP spectra of the former catalyst. It is worth to note that the peak area of Pt $4f_{7/2}$ normalized to that of Pd $3d_{5/2}$ is higher for Pt(Pd/C) than for Pt-Pd/C. This result indicates that the Pt(Pd/C) has higher Pt concentration on its surface than the Pt-Pd/C. It is known that the stand-

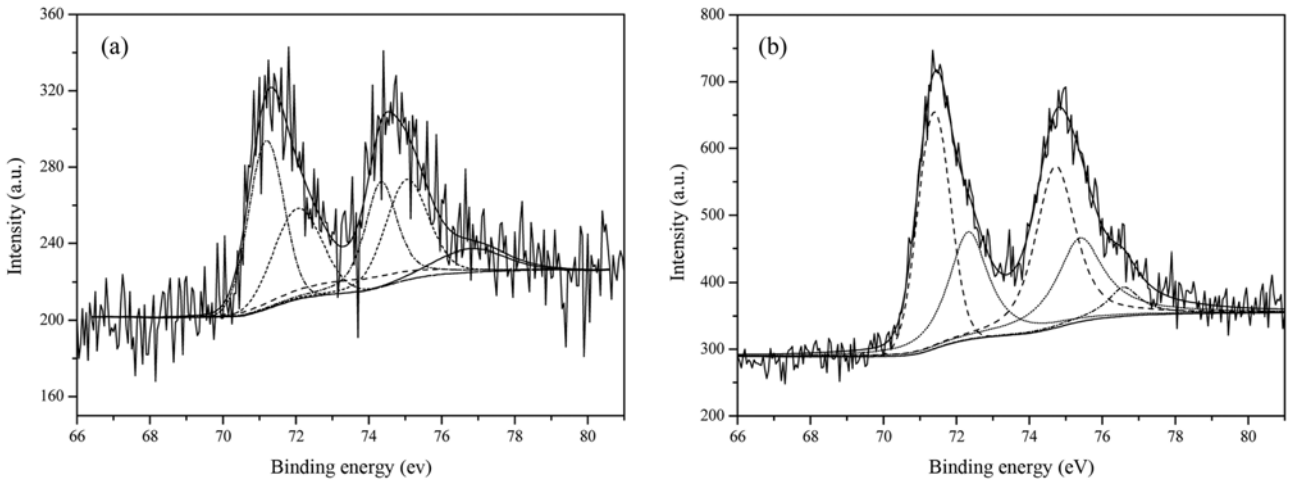

Fig. 3. Pt 4f photoelectron lines for (a) Pt-Pd/C and (b) Pt(Pd/C).

Table 2. Summary of fitting results for Pt 4f photoelectron lines

	Species	Binding energy (eV)	Relative intensity (%)	Relative peak area (%)[a]
Pt-Pd/C	0	71.2	45	9.1
	2+	72.0	40	
	4+	72.9	15	
Pt(Pd/C)	0	71.4	55	18.9
	2+	72.3	40	
	4+	73.2	5	

[a]Normalized area of Pt $4f_{7/2}$ to that of Pd $3d_{5/2}$

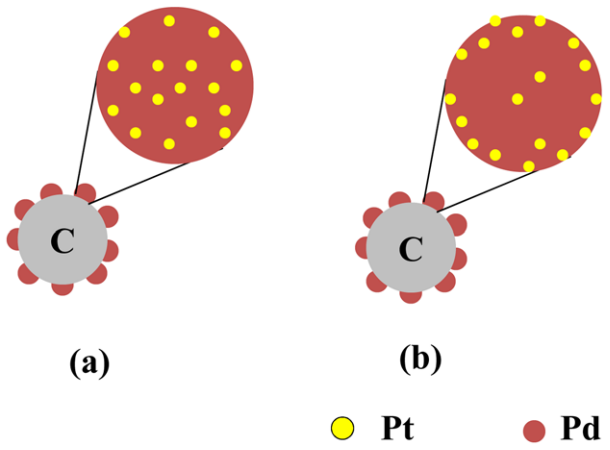

Fig. 4. Schematics for the description of bimetallic composition; (a) Pt-Pd/C and (b) Pt(Pd/C).

ard potentials for the $[PdCl_4]^{2-}$/Pd and $[PtCl_4]^{2-}$/Pt are 0.623 V and 0.758 V [19], respectively, indicating that the Pt precursor would be more easily reduced than Pd precursor. In other words, Pt precursor tends to be reduced to form a Pt-rich core, followed by the reduction of Pd precursor to form a Pd-rich shell, when the reductions are simultaneously carried out in a mixed solution of two metal precursors. Considering an extremely low concentration of Pt precursor in this work, however, the core of Pt-Pd/C is unlikely to be a Pt-rich phase; on the contrary, it seems that a Pd-rich core is first formed followed by the formation of a Pt-rich phase. This does not indicate that the surface of Pt-Pd/C is mainly composed of Pt; instead, it is reasonable to take the view that most of Pt would be residing in the bulk phase rather than on the surface, as illustrated in Fig. 4. In case of Pt(Pd/C), it is possible that some of the Pt is in a separate existence apart from the Pd/C, but most of the Pt is likely to be placed on the surface of Pd as a form of thin layer, which is supported by XPS result and by the analyses of metal particle size.

2. Electrochemical Characterization and ORR Performance

Fig. 5 shows the cyclic voltammograms for the catalysts measured at 10^{th} cycle in N_2-purged 0.5 M H_2SO_4 solution. A common feature of all catalysts in the forward sweep is the evolution of currents for hydrogen desorption and oxide formation, while the current for the reduction of surface oxide and hydrogen adsorption would be observed in the reverse sweep. Based on the charge transferred for hydrogen adsorption or desorption, the electrochemically active surface area (EAS) for Pt/C catalyst was calculated to be 57.4 m^2/g. As far as Pd-based catalyst is involved, it is known that the hydrogen adsorption is concurrent with hydrogen absorption in the same potential region, which makes it impossible to determine the charge density value for the calculation of EAS [20]. Alternatively, one of the most widely accepted methods for the estimation of EAS of Pd is to use the charge transferred for the reduction of PdO, for which the potential range should be controlled to form the monolayer of PdO [20]. Although the experimental condition in this work might be unsuitable for the calculation of real EAS, it would be possible to use the charge value for the reduction of PdO with the aim of a simple comparison of EAS [21]. As listed in Table 1, the reduction charge of PdO per unit mass is decreased in the following order: Pt-Pd/C>Pd/C>Pt(Pd/C), which is in agreement with the results from XRD and TEM.

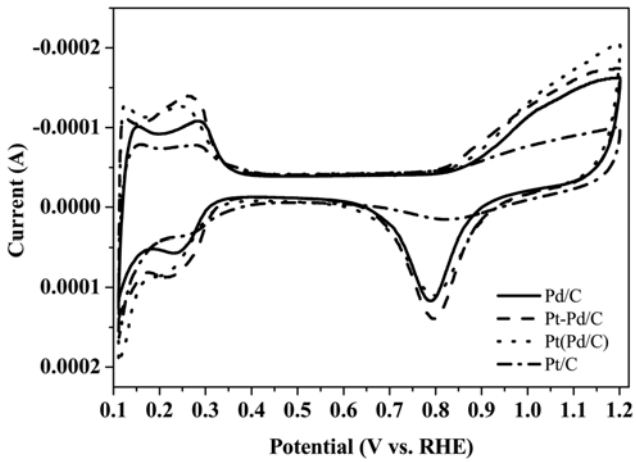

Fig. 5. Cyclic voltammograms with the catalysts in N_2-saturated 0.5 M H_2SO_4 solution. Scan rate: 50 mV/s.

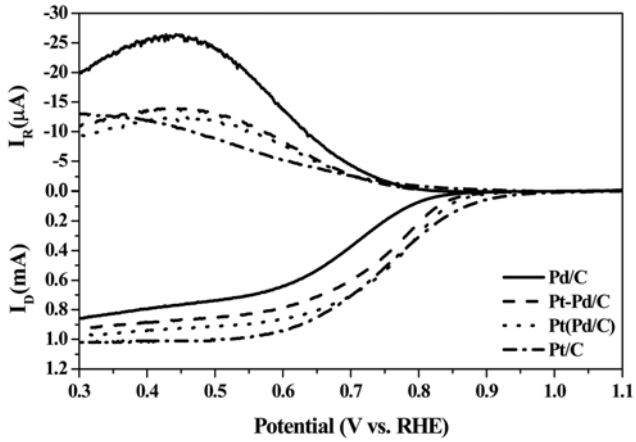

Fig. 6. Linear sweep voltammograms obtained with the catalysts in O_2-saturated 0.5 M H_2SO_4 solution. Rotating speed of 1,600 rpm; Scan rate of 5 mV/s; fixed ring potential at 1.3 V.

To evaluate ORR performances of catalysts, the polarization curves including ring currents were obtained with an RRDE in O_2-saturated 0.5 M H_2SO_4 solution, as presented in Fig. 6. The fraction of peroxide, X_{H2O2}, was calculated by using following equation: $X_{H2O2}=(2I_R/N)/(I_D+I_R/N)$, where I_R, I_D, and N represent ring current, disk current, and collection efficiency (N=0.37), respectively. For all the catalysts, the value of X_{H2O2} at the kinetically controlled poten-

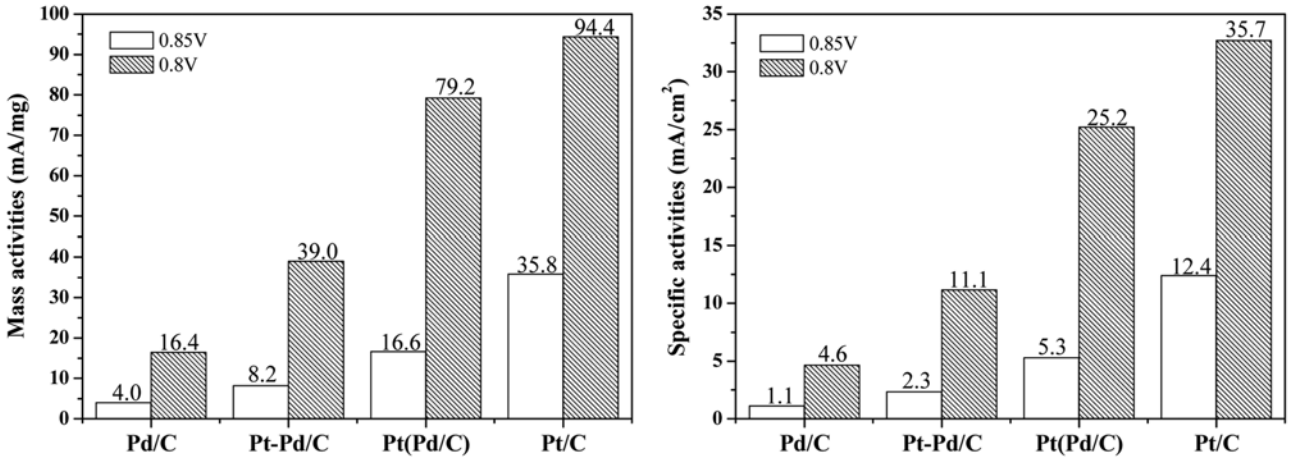

Fig. 7. (a) Mass and (b) specific activities at 0.85 V and 0.8 V.

tial (above 0.7 V) was evaluated to be less than 2%. This result indicates that the ORR involves four-electron transfer on these catalysts, forming water. The ORR performance in terms of ring current (proportional to the fraction of hydroxide formation) and onset potential is enhanced in the order of Pd/C<Pt-Pd/C<Pt(Pd/C)<Pt/C. In addition, it is worthwhile to compare the mass (the kinetic currents normalized to overall metal loadings) and specific activities (the kinetic currents normalized to the surface area) at fixed potentials (0.8 V and 0.85 V), as shown in Fig. 7. The kinetic current was calculated by using the following equation: $i_k=(i_L \times i)/(i_L-i)$, where i_k, i_L, and i represent the kinetic current, limiting current, and measured current, respectively. The surface area obtained from XRD measurement was used for the evaluation of specific activity. The Pt/C shows the highest activity, while the Pd/C has the lowest. Bimetallic catalysts exhibit lower activities than Pt/C. When considering very low activity of Pd/C, however, an enhancement in activity would be achieved by the addition of small amount of Pt to Pd/C. It should be noted that although the nominal Pt concentrations are identical in bimetallic catalysts, the Pt(Pd/C) is observed to have higher activity than Pt-Pd/C; more than two times higher activity in terms of both mass and specific activity at the potentials examined. The large enhancement of catalytic activity on Pt(Pd/C) with respect to Pt-Pd/C as well as Pd/C is believed to have resulted from the Pt rich surface, as confirmed by XPS analyses.

CONCLUSIONS

Two Pd-based PtPd bimetallic samples supported on carbon were prepared by a co-impregnation (Pt-Pd/C) and a sequential impregnation [Pt(Pd/C)] method, and applied as an electro-catalyst for ORR. Depending on the catalyst preparation method, a different surface composition was obtained on each bimetallic catalyst. Due to higher standard potential of Pt precursor compared to Pd precursor, most of the Pt in the Pt-Pd/C was believed to be in the bulk phase of Pd, while the surface of Pt(Pd/C) was likely rich in Pt.

Although bimetallic catalysts showed lower activity than Pt/C, the addition of small amount of Pt to Pd/C was effective to obtain a catalyst with an enhanced ORR activity when considering a low activity of Pd/C. Compared to the Pt-Pd/C, the Pt(Pd/C) had higher ORR performance in terms of both mass activity and specific activity. This was believed to result from the Pt-rich surface on Pt(Pd/C).

ACKNOWLEDGEMENTS

This work was financially supported by the Korean Ministry of Knowledge Economy through the New and Renewable Energy Center under contract number 2008-N-FC08-P-01-0-000. This paper was partly supported by research funds of Chonbuk National University in 2006. We thank Jeonju branch of KBSI for XPS measurement and Mr. J. G. Kang at the Center for University Research Facility for his assistance in the measurement of TEM images.

REFERENCES

1. B. C. H. Steele, A. Heninzel, *Nature*, **414**, 345 (2001).
2. H. I. Joh, S. J. Seo, H. T. Kim and S. H. Moon, *Korean J. Chem. Eng.*, **27**, 45 (2010).
3. V. R. Stamenkovic, B. Fowley, B. S. Mun, G. Wang, P. N. Ross, C. A. Lucas and N. M. Markovic, *Sci.*, **315**, 493 (2007).
4. A. Fuerte, A. Corma, M. Iglesias, E. Morales and F. Sanchez, *Catal. Lett.*, **101**, 99 (2005).
5. R. Bashyam and P. Zelenay, *Nature*, **443**, 63 (2006).
6. Y. Shao, J. Sui, G. Yin and Y. Gao, *Appl. Catal. B*, **79**, 89 (2008).
7. K. I. Tanaka, M. Shou, H. He, C. Zhang and D. Lu, *Catal. Lett.*, **127**, 148 (2009).
8. J. B. Joo, Y. J. Kim, W. Y. Kim, N. D. Kim, P. Kim, Y. H. Kim, Y. W. Lee and J. H. Yi, *Korean J. Chem. Eng.*, **25**, 431 (2008).
9. N. Wakabayashi, M. Takeichi, H. Uchida and M. Watanabe, *J. Phys. Chem. B*, **109**(12), 5836 (2005).
10. J. Shim, C. R. Lee, H. K. Lee, J. S. Lee and E. J. Cairns, *J. Power Sources*, **102**, 172 (2001).
11. P. Mani, R. Srivastava and P. Strasser, *J. Phys. Chem. C*, **112**(7), 2770 (2008).
12. T. Toda, H. Igarashi, H. Uchida and M. Watanabe, *J. Electrochem. Soc.*, **146**(10), 3750 (1999).
13. J. H. Choi, S. Y. Noh, S. D. Han, S. K. Yoon, C. S. Lee, T. S. Hwang and Y. W. Rhee, *Korean J. Chem. Eng.*, **25**, 1026 (2008).
14. J. Zhang, M. B. Vukmirovic, K. Sasaki, A. U. Nilekar, M. Mavrikakis

and R. R. Adzic, *J. Am .Chem. Soc.*, **127**(36), 12480 (2005).
15. W. Wang, Q. Huang, J. Liu, Z. Zou, Z. Li and H. Yang, *Electrochemistry Communications*, **10**, 1396 (2008).
16. J. B. Joo, Y. J. Kim, W. Y. Kim, N. D. Kim, P. Kim, Y. H. Kim and J. H. Yi, *Korean J. Chem. Eng.*, **25**, 770 (2008).
17. A. S. Arico, A. K. Shukla, H. Kim, S. Park, M. Min and V. Antonucci, *Appl. Surf. Sci.*, **172**, 33 (2001).
18. J. Prabhuram, X. Wang, C. L. Hui and I. M. Hsing, *J. Phys. Chem. B*, **107**, 11057 (2003).
19. A. J. Bard, R. Parsons and J. Jordan, *Standard potential in aqueous solution*, Marcel Dekker, New York (1985).
20. M. Grden, M. Lukaszewski, G. Jerkiewicz and A. Czerwinski, *Electrochimica Acta*, **53**, 7583 (2008).
21. H. Liu and A. Manthiram, *Electrochemistry Communications*, **10**, 740 (2008).